

A Non-Quadratic Yield Function for Polymeric Foams

D.-A. Wang^a and J. Pan^{b,*}

^a*Mechanical & Automation Engineering, Da-Yeh University, Chang-Hua 515, Taiwan, ROC*

^b*Mechanical Engineering, The University of Michigan, Ann Arbor, MI 48109-2125, USA*

March 28, 2005

Abstract

The yield behavior of a closed cell polymeric foam is investigated under multiaxial loadings. A phenomenological yield function is developed to characterize the initial yield behavior of the closed cell polymeric foam under a full range of loading conditions. The principal stresses of a relative stress tensor and the second invariant of the deviatoric stress tensor are the main parameters in the yield function. The yield function is a linear combination of non-quadratic functions of the relative principal stresses and the second invariant of the deviatoric stress tensor. The convexity of the yield surface based on the non-quadratic yield function is proved. The non-quadratic yield function is shown to well characterize the yield behavior of a closed cell polymeric foam in Deshpande and Fleck (2001) under a full range of loading conditions. Finally, a comparison of different phenomenological yield functions to characterize the yield behavior of the foam is presented.

Keywords: Yield behavior; Foam; Yield function; Multiaxial loading

* Corresponding author: Tel.:+1-734-764-9404; fax:+1-734-647-3170

E-mail address: jwo@umich.edu (J. Pan).

1. Introduction

Applications of foams are found in many industries for their properties of low densities, low thermal conductivity, high sound absorption and large compressive strains. Polymeric structural foams have been applied to sandwich structures and automotive parts to improve stiffness, durability and crashworthiness with potential benefits of light weight and cost saving (Yamashita et al., 1997; Alwan et al., 2000; Ishida et al., 2001; Pan et al., 2002). Rigid closed cell polyurethane foams are frequently used as an impact energy absorber and as insulation in case of a hypothetical fire accident in plutonium shipping casks (Maji et al., 1995). Syntactic foams, made by a polymeric matrix filled with hollowed spherical inclusions, have been used for ablative heat shields of re-entry vehicles in the aerospace industry, and as structural components such as hulls and bulkheads of ships and submarines (Bardella and Genna, 2001). A hydroxyapatite foam was used for bone implants due to its high biocompatibility and its capability for the penetration of bone into the implant leading to a secure, mechanically stable and integrated implant (Callcut and Knowles, 2002).

In order to determine the maximum load carrying capacity of foams or foam-reinforced structures, the yield or failure behavior of foams needs to be characterized accurately. The yield or failure behavior of foams has been studied by various investigators recently (Gibson et al., 1989; Triantafillou et al., 1989; Bilkhu et al., 1993; Schreyer et al., 1994; Nusholtz et al., 1996; Gibson and Ashby, 1997; Zhang et al., 1997; Chen and Lu, 2000; Deshpande and Fleck, 2000, 2001; Gdoutos et al., 2002; Zhang and Lee, 2003; Doyoyo and Wierzbicki, 2003). Since foams are pressure-sensitive and plastically compressible, a pressure sensitive yield function should be used to model their yield behavior. For pressure-sensitive materials, the second invariant of the deviatoric

stress tensor and the first invariant of the stress tensor (or the mean stress) are usually the two main parameters considered in the yield or failure function.

From the phenomenological viewpoint, Drucker and Prager (1952) proposed a pressure-sensitive yield criterion which is a linear combination of the Mises stress (or the square root of the second invariant of the deviatoric stress tensor) and the mean stress. For modeling of the yield or failure behavior of composites, a yield criterion based on a general quadratic function of stresses was proposed by Tsai and Wu (1971). The Tsai-Wu yield or failure criterion has recently been adopted to describe the yield behavior of foams in Gdoutos et al. (2002). Similarly, Bilkhu et al. (1993) and Nusholtz et al. (1996) proposed a quadratic yield function with a compact form in terms of the Mises stress and the mean stress for polymeric foams. Recently, Doyoyo and Wierzbicki (2003) proposed a quadratic yield function in terms of the second invariant of the deviatoric stress tensor and the first invariant of the stress tensor. The yield function of Doyoto and Wierzbicki (2003) can be shown to be equivalent to that of Bilkhu et al. (1993) and Nusholtz et al. (1996). These yield or failure functions mentioned are quadratic functions of the stresses.

From the mechanism viewpoint, Gibson et al. (1989) developed a yield or failure surface representing the inner envelope of the yield or failure surfaces based on the mechanisms of cell wall bending for deviatoric loading and cell wall stretching for hydrostatic loading. They also analyzed the elastic buckling of cell walls and added a buckling cap to the yield surface. The yield surface with a buckling cap can be used to fit the experimental data under compression and shear dominant loading conditions (Triantafillou et al., 1989). Based on the yield surface with a buckling cap of Gibson et al. (1989), Puso and Govindjee (1995) developed a constitutive law for foams for

implementation into a commercial finite element code with a non-associated flow rule to account for the observed nearly zero plastic Poisson's ratio under compression dominant loading conditions.

Deshpande and Fleck (2000, 2001) proposed a phenomenological yield function for foams based on their experimental observations. Although their quadratic yield function fits well the experimental data under tension and shear dominant loading conditions, a buckling cap based on a maximum compressive principal stress yield criterion is needed to fit the experimental data under compression dominant loading conditions. With consideration of the buckling cap as the yield surface, Deshpande and Fleck (2001) can predict correctly a plastic Poisson's ratio of zero under uniaxial compression based on the associated flow rule in contrast to the use of non-associated flow rules in Puso and Govindjee (1995) and Zhang et al. (1997). It should be noted that Jeong and Pan (1995) and Jeong (2002) proposed yield functions for porous plastics based on their computational results. However, the yield functions have not been validated for closed cell foams with relatively large void volume fractions. Based on the upper bound analysis of Gurson (1977), Zhang and Lee (2003) developed a yield function to describe the yield behavior of open cell foams. Recently, Aubertin and Li (2004) developed a yield function to describe the yielding and failure behaviors of engineering porous materials. Wang and McDowell (2005) derived initial yield functions for metal honeycombs with consideration of cell failure by plastic yielding.

From the phenomenological viewpoint, for dense metallic materials, non-quadratic yield functions were proposed to characterize the yield behavior under multiaxial loading conditions, for example, see Hershey (1954), Hosford (1972), Hill

(1979), Logan and Hosford (1980), Barlat et al. (1989, 1991, 1993, 1997, 2003, 2005), Karafillis and Boyce (1993), Yoon et al. (2000, 2004), Bron and Besson (2004), Cazacu and Barlat (2004), and Hu (2005). Higher order terms of the stresses in these yield functions are needed to characterize the observed flatness and rounded vertices of the yield surface in the stress space. For polymeric foams, Shaw and Sata (1966), Patel (1969) and Zaslavsky (1973) suggested a maximum principal stress yield criterion. Therefore, it is logical to consider a yield function in terms of higher order terms of the stresses to characterize the flat portion of the yield surface based on a maximum principal stress yield criterion for foams from the phenomenological viewpoint. Computationally, the existence of sharp corners or vertices of yield or potential surfaces can result in numerical difficulties in determining the plastic flow in finite element simulations, for example, see Chou et al. (1994). Therefore, the sharp intersections of multiple yield surfaces of Gibson et al. (1989), Deshpande and Fleck (2001), and Puso and Govindjee (1995) can result in numerical difficulties in finite element simulations. On the other hand, numerical difficulties still exist for the higher order yield function of Barlat et al. (1997) in finite element simulations under full stress states (Barlat et al., 2003). However, under plane stress conditions, the higher-order yield functions of Barlat et al. (1997, 2003) do not appear to encounter any numerical difficulties in finite element simulations.

In this paper, a phenomenological yield function is developed to characterize the initial yield behavior of a closed cell polymeric foam under a full range of loading conditions. The goal is to develop a single yield function to describe the yield or failure behavior of the foam instead of multiple yield functions under different loading conditions proposed by Gibson et al. (1989) and Deshpande and Fleck (2001). The

principal stresses of a relative stress tensor and the second invariant of the deviatoric stress tensor are the main parameters in the yield function. The yield function is a linear combination of non-quadratic functions of the relative principal stresses and the second invariant of the deviatoric stress tensor. The convexity of the yield surface based on the non-quadratic yield function is investigated. The non-quadratic yield function is used to characterize the yield behavior of a closed cell PVC (polyvinylchloride) foam (H200) with a density of 200 kg/m^3 , a relative density of 16%, and a cell size of approximately $200 \text{ }\mu\text{m}$ under a full range of loading conditions (Deshpande and Fleck, 2001) to demonstrate the applicability of the yield function. A comparison of different yield functions to characterize the yield behavior of the closed cell foam is also presented.

2. A non-quadratic yield function for isotropic polymeric foams

We propose a non-quadratic isotropic yield function ϕ which is a linear combination of two non-quadratic functions ϕ_1 and ϕ_2 . The function ϕ is expressed as

$$\phi = (1 - \alpha)\phi_1 + \alpha\phi_2 - \bar{\sigma}^m = 0 \quad (1)$$

where α is a fitting parameter with a value between 0 and 1, and $\bar{\sigma}$ is a reference stress.

The two non-quadratic functions ϕ_1 and ϕ_2 are expressed in terms of the relative principal stresses S_1 , S_2 and S_3 as

$$\phi_1 = S_1^m + S_2^m + S_3^m \quad (2)$$

$$\phi_2 = \left\{ \left[\frac{(S_1 - S_2)^2 + (S_2 - S_3)^2 + (S_3 - S_1)^2}{2} \right]^{1/2} \right\}^m \quad (3)$$

The relative principal stresses S_1 , S_2 and S_3 are defined as

$$\begin{aligned}
S_1 &= \sigma_1 - b \\
S_2 &= \sigma_2 - b \\
S_3 &= \sigma_3 - b
\end{aligned}
\tag{4}$$

where σ_1 , σ_2 and σ_3 are the principal stresses of the stress tensor. Here, b is a fitting parameter needed to model the different yield behaviors under tension and compression.

The exponent m in Equations (1), (2) and (3) should depend on the foam considered but needs to be an even integer greater than or equal to 2 to ensure the convexity of the yield function. When $m=2$, the yield function ϕ in Equation (1), which becomes a linear and quadratic combination of the principal stresses, can be reduced to the Tsai-Wu yield criterion (Tsai and Wu, 1971) and a yield function proposed by Bilkhu et al. (1993) and Nusholtz et al. (1996). When $m \rightarrow \infty$ and $\alpha = 0$, the yield function ϕ in Equation (1) corresponds to a maximum principal stress yield criterion. Note that Shaw and Sata (1966), Patel (1969) and Zaslowsky (1973) suggested a maximum principal stress yield criterion to fit their experimental data for the yield of polymeric foams. When $m=2$ and $\alpha=1$, the yield function ϕ in Equation (1) corresponds to the Mises yield criterion. Note that the yield surfaces of Gibson et al. (1989) and Deshpande and Fleck (2001) include flat buckling caps to fit the experimental data. A large value of m is therefore needed to give nearly flat portions of the yield surface based on the proposed yield function ϕ to fit the buckling caps under compression dominant loading conditions. Note that Hershey (1954), Hosford (1972), Hill (1979), Logan and Hosford (1980), Karafillis and Boyce (1993), and Barlat et al. (1997) proposed non-quadratic yield functions with the exponent m not equal to 2 to fit the yield behavior of incompressible polycrystalline metals. It should be noted here that

the non-quadratic yield function proposed by Karafillis and Boyce (1993) is a linear combination of non-quadratic functions of the Mises yield function and the upper bound yield function based on the principal values of the deviatoric stress tensor (Mendelson, 1968). Here, the proposed non-quadratic yield function ϕ for foams is a linear combination of a non-quadratic function ϕ_1 of the relative principal stresses for the nearly flat portion of the yield surface under compression dominant loading conditions and a non-quadratic function ϕ_2 of the second invariant of the deviatoric stress tensor for the portion of the yield surface under shear dominant loading conditions. Note that the third invariant of the deviatoric stress tensor can be incorporated into pressure-sensitive yield functions, for example, see Lee and Ghosh (1996) and Rizzi et al. (2000). In the proposed yield function ϕ , the fitting parameter b is used to model the different yield behaviors of foams under tension and compression loading conditions.

Since the experimental results for a PVC foam (H200) in Deshpande and Fleck (2001) are used as a guide to develop the yield function, we consider the axisymmetric loading conditions as in Deshpande and Fleck (2001). Figure 1 shows a circular cylindrical foam specimen and a Cartesian coordinate system. For simplicity, the value of the exponent m is pre-selected as 8 for the PVC foam. Then the three fitting parameters α , b and $\bar{\sigma}$ can be determined by the yield strengths under three different loading conditions. However, Deshpande and Fleck (2001) provided the yield strengths for the PVC foam under a full range of loading conditions. Note that the PVC foam can be treated as a transversely isotropic material with the normal anisotropic axis in the X_3 direction. We selected nine different yield strengths under different loading conditions to conduct a parametric study to fit the experimental data. These nine strengths are the

hydrostatic compressive strength σ_{hc} , the in-plane balanced biaxial compressive strength σ_{bc} ($=\sigma_1 = \sigma_2$), the in-plane uniaxial compressive strength $(\sigma_c)_1$, the out-of-plane uniaxial compressive strength $(\sigma_c)_3$, the axisymmetric shear strength τ_s , the in-plane uniaxial tensile strength $(\sigma_t)_1$, the out-of-plane uniaxial tensile strength $(\sigma_t)_3$, the in-plane balanced biaxial tensile strength σ_{bt} ($=\sigma_1 = \sigma_2$), and the hydrostatic tensile strength σ_{ht} . The values of these yield strengths in terms of MPa for the PVC foam are listed in Table 1.

Based on a parametric study, at least five yield strengths should be selected and three of them must be σ_{hc} , τ_s and σ_{ht} in order to fit the experimental data reasonably well for the PVC foam under different loading conditions. Note that the axisymmetric shear strength τ_s is defined by the stress state $(-\tau_s/\sqrt{2}, -\tau_s/\sqrt{2}, \sqrt{2}\tau_s)$ under axisymmetric loading conditions. Using the five yield strengths, σ_{hc} , σ_{bc} , $(\sigma_c)_1$, τ_s and σ_{ht} , and substituting the five stress states, $(\sigma_{hc}, \sigma_{hc}, \sigma_{hc})$, $(\sigma_{bc}, \sigma_{bc}, 0)$, $((\sigma_c)_1, 0, 0)$, $(-\tau_s/\sqrt{2}, -\tau_s/\sqrt{2}, \sqrt{2}\tau_s)$ and $(\sigma_{ht}, \sigma_{ht}, \sigma_{ht})$, into Equation (1), we have five independent equations with three unknowns α , b and $\bar{\sigma}$.

In order to fit a non-quadratic yield surface, a large value of m can be pre-selected, as discussed in Karafillis and Boyce (1993). We adopt the same strategy. However, we have conducted a parametric study with $m=2, 6, 8, 12$, and 24 . A comparison of the yield surfaces based on $m=2, 6, 8, 12$ and 24 indicates that the yield surface based on $m=8$ can fit the experimental data better. A nonlinear least squares method was used to find the three fitting parameters, α , b and $\bar{\sigma}$, to fit the five independent equations. The nonlinear least squares method gives a minimum of the sum

of the squares of the functions based on the five independent equations. The five independent equations for determination of these fitting parameters can be found in Appendix A. Note that the solutions based on the nonlinear least squares method are non-unique. Different sets of the fitting parameters can be obtained depending upon different initial guesses. Based on a parametric study, if the initial guesses of the fitting parameters b and $\bar{\sigma}$ are any real numbers between -30 and 90, and the initial guess of the fitting parameter α is any real number between 0 and 1, all the solutions obtained are nearly the same. The set of the fitting parameters α , b and $\bar{\sigma}$ that we found for $m = 8$ is listed in Table 2.

2.1 Yield surfaces based on the non-quadratic isotropic yield function ϕ

The yield surface of the foam based on the isotropic yield function ϕ with the three fitting parameters, α , b and $\bar{\sigma}$, is plotted in Figure 2 in terms of the principal stresses σ_1 , σ_2 and σ_3 . The commercial surface modeling software SURFACER is employed to generate the three-dimensional yield surface. Figure 2 shows the yield surface in the principal stress space. Some nearly flat portions of the yield surface for $\sigma_1 > 0$, $\sigma_2 > 0$ and $\sigma_3 > 0$ and for $\sigma_1 < 0$, $\sigma_2 < 0$ and $\sigma_3 < 0$ are marked in the figure. The nearly flat portions of the yield surface are similar to the parts of the yield surface based on the maximum principal stress yield criterion. Figure 2 also shows the cylinder-like portion of the yield surface parallel to the hydrostatic stress axis $\sigma_1 = \sigma_2 = \sigma_3$. This portion of the yield surface is similar to that based on the Mises yield criterion. The hydrostatic stress axis $\sigma_1 = \sigma_2 = \sigma_3$ passes the loci of the hydrostatic compressive and tensile yield stress states, $(\sigma_{hc}, \sigma_{hc}, \sigma_{hc})$ and $(\sigma_{ht}, \sigma_{ht}, \sigma_{ht})$, on the yield surface. Note

that the portions of the yield surface with rounded corners or vertices as shown in Figure 2 in the compressions and shear dominant regions represent the stress states that are smoothly connecting the two portions of the yield surfaces based on two different microscopic deformation mechanisms.

The yield surface based on the yield function ϕ and the experimental data of Deshpande and Fleck (2001) are plotted in Figure 3 in terms of σ_1 and σ_3 . As shown in Figure 3, the experimental data are adequately fitted. The yield surface based on the yield function ϕ and the experimental data are plotted in Figure 4 in terms of σ_m and $\sigma_3 - \sigma_1$, where $\sigma_m = (\sigma_1 + \sigma_2 + \sigma_3)/3$. Note that $|\sigma_3 - \sigma_1|$ is the Mises stress under axisymmetric loading conditions. As shown in Figure 4, the experimental data are fitted reasonably well. Figure 5 shows the yield surface based on the yield function ϕ and the experimental data for the foam in terms of σ_1 and σ_3 in the plane of $\sigma_2 = 0$. As shown in Figure 5, the experimental data are fitted reasonably well in this plane. The yield surface based on the yield function ϕ and the experimental data in the plane of $\sigma_2 = 0$ are plotted in Figure 6 in terms of σ_m and $\sigma_3 - \sigma_1$. As shown in Figure 6, the experimental data are also fitted reasonably well.

2.2 Convexity of the non-quadratic isotropic yield function ϕ

We have shown that the yield surface based on the yield function ϕ can fit the experimental data well. The convexity of the yield surface based on the yield function ϕ in the stress space can be proved by proving that the two yield surfaces based on the two yield functions ϕ_1 and ϕ_2 are convex in the stress space. First, we will prove that the

yield surface based on the yield function ϕ_1 in convex. A yield function Ψ is convex if its Hessian matrix H

$$H_{ij} = \frac{\partial^2 \Psi}{\partial \sigma_i \partial \sigma_j} \quad (5)$$

is positive semi-definite (Rockafellar, 1970). The property of the positive semi-definiteness can be proved by showing that the eigenvalues of the Hessian matrix H are non-negative. Since the fitting parameter b in the yield function ϕ contributes to the translation of the yield surface, it can be taken as 0 without changing the convexity of the yield surface. The Hessian matrix H_1 for ϕ_1 with $b = 0$ is

$$H_1 = \begin{bmatrix} m(m-1)\sigma_1^{m-2} & 0 & 0 \\ 0 & m(m-1)\sigma_2^{m-2} & 0 \\ 0 & 0 & m(m-1)\sigma_3^{m-2} \end{bmatrix} \quad (6)$$

The three eigenvalues, $m(m-1)\sigma_1^{m-2}$, $m(m-1)\sigma_2^{m-2}$ and $m(m-1)\sigma_3^{m-2}$, are not negative when m is an even integer greater than or equal to 2.

Similarly, the Hessian matrix H_2 for ϕ_2 with $b = 0$ is

$$H_2 = \begin{bmatrix} \frac{mC_4^{m/2}(mC_1^2 + 4C_4 - 2C_1^2)}{4C_4^2} & \frac{mC_4^{m/2}(mC_1C_2 - 2C_4 - 2C_1C_2)}{4C_4^2} \\ \frac{mC_4^{m/2}(mC_2C_1 - 2C_4 - 2C_2C_1)}{4C_4^2} & \frac{mC_4^{m/2}(mC_2^2 + 4C_4 - 2C_2^2)}{4C_4^2} \\ \frac{mC_4^{m/2}(mC_1C_3 - 2C_4 - 2C_1C_3)}{4C_4^2} & \frac{mC_4^{m/2}(mC_3C_2 - 2C_4 - 2C_3C_2)}{4C_4^2} \\ \frac{mC_4^{m/2}(mC_2C_3 - 2C_4 - 2C_2C_3)}{4C_4^2} & \\ \frac{mC_4^{m/2}(mC_3^2 + 4C_4 - 2C_3^2)}{4C_4^2} \end{bmatrix} \quad (7)$$

where

$$C_1 = 2\sigma_1 - \sigma_2 - \sigma_3 \quad (8)$$

$$C_2 = 2\sigma_2 - \sigma_3 - \sigma_1 \quad (9)$$

$$C_3 = 2\sigma_3 - \sigma_1 - \sigma_2 \quad (10)$$

$$C_4 = \frac{(\sigma_1 - \sigma_2)^2 + (\sigma_2 - \sigma_3)^2 + (\sigma_3 - \sigma_1)^2}{2} \quad (11)$$

The three eigenvalues, 0 , $\frac{3mC_4^{m/2}}{2C_4}$ and $\frac{3m(m-1)C_4^{m/2}}{2C_4}$, are not negative when m is

greater than or equal to 1.

Both ϕ_1 and ϕ_2 are convex in the stress space when m is taken as an even integer greater than or equal to 2. Since the sum of two convex functions is also a convex function (Rockafellar, 1970), the convexity of the yield surface is ensured when m is an even integer greater than or equal to 2. Note that the initial yield surface of the H200 foam appears to be convex based on the experimental data of Deshpande and Fleck (2001).

In general, foams can be idealized as orthotropic materials due to the foaming process. The orthotropy should be taken into account in the formulation of a yield function for foams. Since we have no experimental data for the shear strengths with respect to the orthotropic symmetry planes for the PVC foam (H200), we here develop a special yield function for orthotropic foams under restricted loading conditions without any shear contribution with respect to the orthotropic symmetry planes. The development of the special orthotropic yield function for orthotropic foams is presented in Appendix B.

2.3 Other yield functions

The yield surfaces based on the quadratic yield functions proposed by Bilkhu et al. (1993) and Deshpande and Fleck (2000, 2001) with a buckling cap are also presented here for comparison. Bilkhu et al. (1993) proposed a quadratic yield function ϕ_b in terms of σ_e and σ_m for polymeric foams as

$$\phi_b = \left(\frac{\sigma_e}{\eta} \right)^2 + \left(\frac{\sigma_m - \chi}{\lambda} \right)^2 - 1 = 0 \quad (12)$$

where η , λ and χ are fitting parameters. σ_e and σ_m are the Mises stress and mean stress, respectively. σ_e and σ_m can be expressed in terms of the principal stresses σ_1 , σ_2 and σ_3 as

$$\sigma_e = \left[\frac{(\sigma_1 - \sigma_2)^2 + (\sigma_2 - \sigma_3)^2 + (\sigma_3 - \sigma_1)^2}{2} \right]^{\frac{1}{2}} \quad (13)$$

$$\sigma_m = \frac{\sigma_1 + \sigma_2 + \sigma_3}{3} \quad (14)$$

Here, the three fitting parameters, η , λ and χ , in Equation (12) for the PVC foam are determined by the hydrostatic compressive strength σ_{hc} , the out-of-plane uniaxial tensile strength $(\sigma_t)_3$, and the hydrostatic tensile strength σ_{ht} , as listed in Table 1. The values of these three fitting parameters, η , λ and χ , for the foam are 3.6250 MPa, 4.5558 MPa and 0.5950 MPa, respectively.

A quadratic yield function ϕ_d proposed by Deshpande and Fleck (2000, 2001) is written as

$$\phi_d = \frac{1}{1+(\gamma/3)^2}(\sigma_e^2 + \gamma^2\sigma_m^2) - \sigma_Y^2 = 0 \quad (15)$$

where σ_Y is the uniaxial tensile or compressive strength of a foam, and γ is a fitting parameter. Here, σ_Y is taken as the out-of-plane uniaxial tensile strength $(\sigma_t)_3$ for the foam as listed in Table 1, and the stress state of $\sigma_1 = \sigma_2 = -2.2$ MPa and $\sigma_3 = 2.5$ MPa of the experimental data for the foam is used to determine the fitting parameter γ . The value of γ is determined as 1.2013 for the foam.

Figure 7 shows the yield surfaces in terms of σ_1 and σ_3 based on the function ϕ_b in Equation (12), the function ϕ_d in Equation (15), and the function ϕ in Equation (1). The experimental data and a buckling cap are also shown in the figure. Both quadratic yield functions ϕ_b and ϕ_d cannot fit the yield behavior of the foam under compression dominant loading conditions. A buckling cap based on a maximum principal stress yield criterion, shown as two dotted lines in Figure 7, is needed in order to adequately fit the experimental data. Figure 7 also shows that the function ϕ can fit the experimental data better than the functions ϕ_b and ϕ_d with the additional buckling cap.

Figure 8 shows the yield surfaces based on the functions ϕ_b , ϕ_d , and ϕ in terms of σ_m and $\sigma_3 - \sigma_1$. The experimental data and a buckling cap are also shown in the figure. As shown in the figure, without the additional buckling cap shown as the dotted lines, the functions ϕ_b and ϕ_d alone cannot fit the yield behavior of the foam well under compression dominant loading. On the other hand, the function ϕ can fit the full range of the yield behavior of the foam reasonably well. Note that the yield surface based on

the function ϕ is not symmetric with respect to the σ_m axis whereas the yield surfaces based on the functions ϕ_d and ϕ_b are symmetric with respect to the σ_m axis.

Figure 9 shows the yield surfaces based on the functions ϕ_b , ϕ_d , and ϕ in terms of σ_1 and σ_3 in the plane of $\sigma_2 = 0$. The experimental data and a buckling cap are also shown in the figure. The function ϕ can fit the experimental data better than the functions ϕ_b and ϕ_d alone. However, with consideration of the buckling cap, the yield surfaces based on the functions ϕ_b and ϕ_d can fit the limited experimental data well. The yield surfaces based on the functions ϕ_b , ϕ_d , and ϕ in terms of σ_m and $\sigma_3 - \sigma_1$ in the plane of $\sigma_2 = 0$ are plotted in Figure 10. The experimental data and a buckling cap are also shown in the figure. As shown in the figure, the limited experimental data are fitted well by the function ϕ alone and by the function ϕ_d with a buckling cap. The function ϕ_b , even with a buckling cap, does not seem to fit the limited experimental data well.

2.4 Initial plastic Poisson's ratio

We have shown that the function ϕ can fit the initial yield surface of the foam. Now we need to specify a flow rule in order to examine the plastic Poisson's ratio of the foam under uniaxial compression. Both the associated flow rule and the non-associated flow rule were used in the modeling of the yield behavior of foams in the past. Puso and Govindjee (1995) and Zhang et al. (1997) adopted non-associated flow rules in order to account for the observed nearly zero plastic Poisson's ratio of polymeric foams. However, with consideration of the buckling cap, Deshpande and Fleck (2001) can

predict correctly a plastic Poisson's ratio of zero under uniaxial compression based on the associated flow rule.

The associated flow rule is adopted here to examine the initial plastic Poisson's ratio based on the initial yield surface under uniaxial compression. The associated flow rule can be written as

$$\dot{\varepsilon}_i^p = \dot{\lambda} \frac{\partial \phi}{\partial \sigma_i} \quad (16)$$

where $\dot{\lambda}$ is a scalar factor of proportionality, and $\dot{\varepsilon}_i^p$ and σ_i , with a subscript i ranging from 1 to 3, are the plastic strain rates and the stresses in the principal directions of the stress tensor, respectively. Based on the associated flow rule in Equation (16) and the function ϕ , the plastic Poisson's ratio ν^p for uniaxial compression with $\sigma_1 \neq 0$ and $\sigma_2 = \sigma_3 = 0$ can be expressed as

$$\begin{aligned} \nu^p &= -\frac{d\varepsilon_3^p}{d\varepsilon_1^p} \\ &= \frac{-(1-\alpha)(-b/\sigma_1)^{m-1} + \alpha/2}{(1-\alpha)(1-b/\sigma_1)^{m-1} + \alpha} \end{aligned} \quad (17)$$

As expressed in Equation (17), the plastic Poisson's ratio ν^p is dependent upon m , α and b/σ_1 . When the value of σ_1 is taken as the in-plane uniaxial compressive strength $(\sigma_c)_1$ as listed in Table 1 and the fitting parameters m , α and b are taken as those listed in Table 2, the plastic Poisson's ratio ν^p can be determined to be 0.037. The small value is in agreement with the experimental observations of the nearly zero plastic Poisson's ratio of the foam.

When $\alpha = 1$, the yield function ϕ depends on the second invariant of the deviatoric stress tensor only. As indicated in Equation (17) based on the associated flow rule, the plastic Poisson's ratio for incompressible materials, $\nu^p = 1/2$, is recovered. When $\alpha = 0$, the yield function ϕ is based on the relative principal stresses only. Equation (17) becomes

$$\nu^p = \frac{-(-b/\sigma_1)^{m-1}}{(1-b/\sigma_1)^{m-1}} \quad (18)$$

As indicated in Equation (18), the plastic Poisson's ratio ν^p depends on m and b/σ_1 . When m is selected to be a large even integer and $|b/\sigma_1|$ is selected to be a small value less than 1, the plastic Poisson's ratio should be a small value. When $b = 0$, the plastic Poisson's ratio ν^p is zero.

3. Conclusions and Discussions

A phenomenological non-quadratic yield function is developed here to model the initial yield behavior of a polymeric foam. Different yield behaviors under tension and compression dominant loading due to different yield or failure mechanisms of polymeric foams are taken into account in the yield function. The principal stresses of a relative stress tensor and the second invariant of the deviatoric stress tensor are the main parameters in the yield function. The yield function is a linear combination of non-quadratic functions of the relative principal stresses and the second invariant of the deviatoric stress tensor. The convexity of the yield surface based on the yield function is proved. The yield function is shown to fit the yield surface of the foam under a full range of loading conditions. A comparison of different phenomenological yield functions to fit

the yield surface of the foam is also presented. Note that the proposed yield function is intended to model the initial yield surface with flat portions for closed cell foams. With three fitting parameters and a large exponent, the proposed yield function can be quite flexible to fit yield surfaces with flat portions in compression and tension dominant stress states.

It should be mentioned that a nonlinear least squares method can be used to find better fitting parameters for ϕ_b and ϕ_d . However, these better fitting parameters cannot change significantly the general shapes of the yield surfaces to have nearly flat portions that are needed to represent the experimental data well. Finally, Deshpande and Fleck (2001) presented only a limited number of data points for the PVC foam (H200) under tension dominant loading conditions. Due to the symmetry of the non-quadratic yield function ϕ in Equation (1), the yield surface has also nearly flat portions under tension dominant loading conditions. A quadratic yield function may fit the experimental data well under tension dominant loading conditions. Therefore, the non-quadratic function ϕ in Equation (1) may be used under compression and shear dominant loadings with more confidence. Under tension and shear dominant loading conditions, the yield functions of Bilkhu et al. (1993) and Deshpande and Fleck (2000, 2001) may be used. When tension, compression and shear dominant stress states are involved simultaneously, the non-quadratic yield function ϕ in Equation (1) should be applied with carefully selected fitting parameters that can fit the general shape of the yield surface under tension, compression and shear loading conditions.

Acknowledgement

The support of this work by a grant from Ford Motor Company is greatly appreciated. Helpful discussions with F. Barlat of Alcoa and J. W. Yoon of MSC Software are greatly appreciated. The authors are also thankful for valuable suggestions from W. F. Hosford of the Department of Materials Science and Engineering of University of Michigan in drafting of this paper.

Appendix A: Equations to determine fitting parameters for isotropic foams

We first consider the case of hydrostatic compression. In this case, $\sigma_1 = \sigma_2 = \sigma_3 = \sigma_{hc}$. The function ϕ in Equation (1) can be expressed as

$$\phi = (1 - \alpha) \left[(\sigma_{hc} - b)^m + (\sigma_{hc} - b)^m + (\sigma_{hc} - b)^m \right] - \bar{\sigma}^m \quad (\text{A1})$$

Next, we consider the case of in-plane balanced biaxial compression. In this case, $\sigma_1 = \sigma_2 = \sigma_{bc}$ and $\sigma_3 = 0$. The function ϕ can be expressed as

$$\phi = (1 - \alpha) \left[(\sigma_{bc} - b)^m + (\sigma_{bc} - b)^m + (-b)^m \right] + \alpha |\sigma_{bc}|^m - \bar{\sigma}^m \quad (\text{A2})$$

Then, we consider the case of in-plane uniaxial compression. In this case, $\sigma_1 = (\sigma_c)_1$ and $\sigma_2 = \sigma_3 = 0$. The function ϕ can be expressed as

$$\phi = (1 - \alpha) \left[((\sigma_c)_1 - b)^m + (-b)^m + (-b)^m \right] + \alpha |(\sigma_c)_1|^m - \bar{\sigma}^m \quad (\text{A3})$$

Now, we consider the case of axisymmetric shear. In this case, $\sigma_1 = \sigma_2$ and $\sigma_1 + \sigma_2 + \sigma_3 = 0$. Therefore, $\sigma_1 = \sigma_2 = -\sigma_3/2$. We can express the principal stresses σ_1 , σ_2 and σ_3 in terms of τ_s . Here, τ_s represents the axisymmetric shear strength as illustrated by the Mohr circle shown in Figure A1. Based on the Mohr circle as shown, $\sigma_1 = \sigma_2 = -\tau_s/\sqrt{2}$ and $\sigma_3 = \sqrt{2}\tau_s$. Therefore, the function ϕ can be expressed as

$$\phi = (1 - \alpha) \left[\left(\frac{-\tau_s}{\sqrt{2}} - b \right)^m + \left(\frac{-\tau_s}{\sqrt{2}} - b \right)^m + \left(\sqrt{2}\tau_s - b \right)^m \right] + \alpha \left(\frac{3\sqrt{2}}{2}\tau_s \right)^m - \bar{\sigma}^m \quad (\text{A4})$$

Finally, we consider the case of hydrostatic tension. In this case, $\sigma_1 = \sigma_2 = \sigma_3 = \sigma_{ht}$.

The function ϕ can be expressed as

$$\phi = (1 - \alpha) \left[(\sigma_{ht} - b)^m + (\sigma_{ht} - b)^m + (\sigma_{ht} - b)^m \right] - \bar{\sigma}^m \quad (\text{A5})$$

Appendix B: A special yield function Φ for orthotropic foams

A special non-quadratic yield function Φ for orthotropic foams with the symmetry axes coinciding with the Cartesian axes x_1 , x_2 and x_3 is proposed as

$$\Phi = (1 - \alpha)\Phi_1 + \alpha\Phi_2 - \bar{\sigma}^m = 0 \quad (\text{B1})$$

where α is a fitting parameter with a value between 0 and 1, and $\bar{\sigma}$ is a reference stress. We consider the stress states with only the normal stresses σ_1 , σ_2 and σ_3 in the x_1 , x_2 and x_3 directions. No shear stresses with respect to the x_1 , x_2 and x_3 axes are considered. The two non-quadratic functions Φ_1 and Φ_2 are expressed in terms of the relative normal stresses Σ_1 , Σ_2 and Σ_3 as

$$\Phi_1 = \Sigma_1^m + \Sigma_2^m + \Sigma_3^m \quad (\text{B2})$$

$$\Phi_2 = \left\{ \left[\frac{(\Sigma_1 - \Sigma_2)^2 + (\Sigma_2 - \Sigma_3)^2 + (\Sigma_3 - \Sigma_1)^2}{2} \right]^{1/2} \right\}^m \quad (\text{B3})$$

The relative normal stresses Σ_1 , Σ_2 and Σ_3 are defined as

$$\begin{aligned} \Sigma_1 &= a_1(\sigma_1 - b_1) \\ \Sigma_2 &= a_2(\sigma_2 - b_2) \\ \Sigma_3 &= a_3(\sigma_3 - b_3) \end{aligned} \quad (\text{B4})$$

where a_1 , a_2 , a_3 , b_1 , b_2 and b_3 are fitting parameters. Here, a_1 , a_2 , a_3 , b_1 , b_2 and b_3 determine the orthotropy of a foam and the center of the yield surface. b_1 , b_2 and b_3 are needed to model the different yield behaviors under tension and compression in the x_1 , x_2 and x_3 directions.

B.1 Determination of fitting parameters

Since the experimental results for a PVC foam (H200) in Deshpande and Fleck (2001) are used as a guide to develop the orthotropic yield function, we here consider the axisymmetric loadings as in Deshpande and Fleck (2001). Figure 1 shows a circular cylindrical foam specimen and a Cartesian coordinate system. The foam is assumed to be isotropic within the $x_1 - x_2$ plane. Normal anisotropy is assumed in the x_3 direction which is taken as the rise direction of the foam. Therefore, we can take $b_1 = b_2$ and $a_1 = a_2 = 1$.

Based on a parametric study, at least six yield strengths should be selected and three of them must be σ_{hc} , τ_s and σ_{ht} to determine the fitting parameters α , a_3 , b ($= b_1 = b_2$), b_3 and $\bar{\sigma}$ in order to fit the experimental data reasonably well for the PVC foam under the restricted loading conditions. Using the six yield strengths, σ_{hc} , $(\sigma_c)_3$, τ_s , $(\sigma_t)_1$, $(\sigma_t)_3$ and σ_{ht} , and substituting the six stress states, $(\sigma_{hc}, \sigma_{hc}, \sigma_{hc})$, $(0, 0, (\sigma_c)_3)$, $(-\tau_s/\sqrt{2}, -\tau_s/\sqrt{2}, \sqrt{2}\tau_s)$, $(0, 0, (\sigma_t)_1)$, $(0, 0, (\sigma_t)_3)$ and $(\sigma_{ht}, \sigma_{ht}, \sigma_{ht})$, into Equation (B1) with $b_1 = b_2 = b$ and $a_1 = a_2 = 1$, we have six independent equations with five unknowns, α , a_3 , b , b_3 and $\bar{\sigma}$. Note that the value of the exponent m is considered as a known value. Here, the exponent m is taken as 8 for the foam. A nonlinear least squares method was used to find the five fitting parameters, α , a_3 , b , b_3 and $\bar{\sigma}$, to fit the six independent equations. A set of the fitting parameters, α , a_3 , b , b_3 and $\bar{\sigma}$, for $m = 8$ was obtained and listed in Table B1.

B.2 Yield surfaces based on the orthotropic yield function Φ

The yield surface of the foam based on the orthotropic yield function Φ with the five fitting parameters, α , a_3 , b , b_3 and $\bar{\sigma}$, the yield surface based on the isotropic yield function ϕ with the three fitting parameters, α , b and $\bar{\sigma}$, and the experimental data of Deshpande and Fleck (2001) are plotted in Figures B1-B4 in terms of the different stresses as in Figures 3-6. Figures B1-B4 show that the experimental data are fitted reasonably well by the functions ϕ and Φ under a full range of loading conditions. As also shown in Figures B1-B4, the yield surfaces based on both functions ϕ and Φ are similar in terms of their shape, size and position. It should be noted that the orthotropy of the foam in terms of different uniaxial strengths in different loading directions as shown in Figures B3 and B4 can be approximated reasonably well by both functions ϕ and Φ .

B-3. Convexity of the orthotropic yield function Φ

In order to prove the convexity of the yield surface based on the orthotropic yield function Φ in the stress space, we need to show that the Hessian matrix H' of the yield function Φ is positive semi-definite (Rockafellar, 1970). The Hessian matrix H' of the function Φ can be written as

$$H'_{ij} = \frac{\partial^2 \Phi}{\partial \sigma_i \partial \sigma_j} \quad (\text{B5})$$

The property of the positive semi-definiteness can be proved by showing that the eigenvalues of the Hessian matrix H' are non-negative. Note that the three fitting parameters, b_1 , b_2 and b_3 , in the function Φ contribute to the translation of the yield surface in the stress space. For simplicity, they can be taken as 0 without changing the

convexity of the yield surface. The Hessian matrix H' for Φ with $b_1 = b_2 = b_3 = 0$ can be written as

$$H'_{ij} = \frac{\partial^2 \Phi}{\partial \sigma_i \partial \sigma_j} = \frac{\partial \Sigma_i}{\partial \sigma_k} \frac{\partial^2 \Phi}{\partial \Sigma_i \partial \Sigma_j} \frac{\partial \Sigma_j}{\partial \sigma_l} \quad (\text{B6})$$

Here, we can define the transformation matrix T_{ij} based on Equation (B4) as

$$T_{ij} = \frac{\partial \Sigma_i}{\partial \sigma_j} = \begin{bmatrix} a_1 & 0 & 0 \\ 0 & a_2 & 0 \\ 0 & 0 & a_3 \end{bmatrix} \quad (\text{B7})$$

For $a_1 > 0$, $a_2 > 0$ and $a_3 > 0$, the transformation matrix is positive definite. We have

shown that $\frac{\partial^2 \phi}{\partial \sigma_i \partial \sigma_j}$ for the function ϕ is positive semi-definite when m is an even

integer greater than or equal to 2. Since Φ has the same functional form with respect to

Σ_1 , Σ_2 and Σ_3 as ϕ to σ_1 , σ_2 and σ_3 , $\frac{\partial^2 \Phi}{\partial \Sigma_i \partial \Sigma_j}$ is positive semi-definite. According to

Equation (B6) with the positive definite matrix T_{ij} , H'_{ij} is positive semi-definite when m

is an even integer greater than or equal to 2. Therefore, the yield surface based on the

function Φ is convex when m is an even integer greater than or equal to 2.

References

- Aubertin, M., Li, L., 2004. A porosity-dependent inelastic criterion for engineering materials. *International Journal of Plasticity* 20, 2179-2208.
- Alwan, J. M., Wu, C.-C., Chou, C. C., 2000. Effect of polyurethane foam on the energy management of structural components. SAE Technical Paper 2000-01-0052, Society of Automotive Engineers, Warrendale, Pennsylvania.
- Bardella, L., Genna, F., 2001. On the elastic behavior of syntactic foams. *International Journal of Solids and Structures* 38, 7235-7260.
- Barlat, F., Lian, J., 1989. Plastic behavior and stretchability of sheet metals. Part I: a yield function for orthotropic sheets under plane stress conditions. *International Journal of Plasticity* 5, 51-66.
- Barlat, F., Lege, D. J., Brem, J. C., 1991. A six-component yield function for anisotropic materials. *International Journal of Plasticity* 7, 693-712.
- Barlat, F., Chung, K., Richmond, O., 1993. Strain rate potential for metals and its application to minimum plastic work path calculations. *International Journal of Plasticity* 9, 51-63.
- Barlat, F., Maeda, Y., Chung, K., Yanagawa, M., Brem, J. C., Hayashida, Y., Lege, D. J., Matsui, K., Murtha, S. J., Hattori, S., Becker, R. C., Makosey, S., 1997. Yield function development for aluminum alloy sheets. *Journal of the Mechanics and Physics of Solids* 45, 1727-1763.
- Barlat, F., Brem, J. C., Yoon, J. W., Chung, K., Dick, R. E., Lege, D. J., Pourboghrat, F., Choi, S.-H., Chu, E., 2003. Plane stress yield function for aluminum alloy sheets – part 1: theory. *International Journal of Plasticity* 19, 1297-1319.
- Barlat, F., Aretz, H., Yoon, J.-W., Karabin, M. E., Brem, J. C., Dick, R. E., 2005. Linear transformation-based anisotropic yield functions. *International Journal of Plasticity* 21, 1009-1039.

- Bilkhu, S. S., Founas, M., Nusholtz, G. S., 1993. Material modeling of structural foams in finite element analysis using compressive uniaxial and triaxial data. SAE Technical Paper 930434, Society of Automotive Engineers, Warrendale, Pennsylvania.
- Bron, F, Besson, J., 2004. A yield function for anisotropic materials Application to aluminum alloys. *International Journal of Plasticity* 20, 937-963.
- Callcut, S., Knowles, J. C., 2002. Correlation between structure and compressive strength in a reticulated glass-reinforced hydroxyapatite foam. *Journal of Materials Science: Materials in Medicine* 13, 485-489.
- Cazacu, O., Barlat, F., 2004. A criterion for description of anisotropy and yield differential effects in pressure-insensitive metals. *International Journal of Plasticity* 20, 2027-2045.
- Chen, C., Lu, T. J., 2000. A phenomenological framework of constitutive modelling for incompressible and compressible elasto-plastic solids. *International Journal of Solids and Structures* 37, 7769-7786.
- Chou, C. H., Pan, J., Tang, S. C., 1994. Analysis of sheet metal forming operations by a stress resultant constitutive law. *International Journal for Numerical Methods in Engineering* 37, 717-735.
- Deshpande, V. S., Fleck, N. A., 2000. Isotropic constitutive models for metallic foams. *Journal of the Mechanics and Physics of Solids* 48, 1253-1283.
- Deshpande, V. S., Fleck, N. A., 2001. Multi-axial yield behavior of polymer foams. *Acta Materialia* 49, 1859-1866.
- Doyoyo, M., Wierzbicki, T., 2003. Experimental studies on the yield behavior of ductile and brittle aluminum foams. *International Journal of Plasticity* 19, 1195-1214.
- Drucker, D. C., Prager, W., 1952. Soil mechanics and plastic analysis or limit design. *Quarterly Applied Mathematics* 10, 157-165.
- Gdoutos, E. E., Daniel, I. M., Wang, K.-A., 2002. Yield of cellular foams under multiaxial loading. *Composites: Part A* 33, 163-176.

- Gibson, L. J., Ashby, M. F., Zhang, J., Triantafillou, T. C., 1989. Yield surfaces for cellular materials under multiaxial loads – I. modeling. *International Journal of Mechanical Sciences* 31, 635-663.
- Gibson, L. J., Ashby, M. F., 1997. *Cellular solids: structure and properties*. Second edition, Cambridge University Press, Cambridge, UK.
- Gurson, A. L., 1977. Continuum theory of ductile rupture by void nucleation and growth: part I – yield criteria and flow rules for porous ductile media. *Journal of Engineering Materials and Technology* 99, 2-15.
- Hershey, A. V., 1954. The plasticity of an isotropic aggregate of anisotropic face-centered cubic crystals. *Journal of Applied Mechanics* 76, 241-249.
- Hill, R., 1979. Theoretical plasticity of textured aggregates. *Mathematical Proceedings of the Cambridge Philosophical Society* 85, 179-191.
- Hosford, W. F., 1972. A generalized isotropic yield criterion. *Journal of Applied Mechanics* 69, 607-609.
- Hu, W., 2005. An orthotropic yield criterion in a 3-D general stress state. *International Journal of Plasticity*, in press.
- Ishida, K., Fukahori, M., Hanakawa, K., Tanaka, H., Matsuda, K., 2001. Development of a technique to strengthen body frame with structural foam. SAE Technical Paper 2001-01-0313, Society of Automotive Engineers, Warrendale, Pennsylvania.
- Jeong, H.-Y., Pan, J., 1995. A macroscopic constitutive law for porous solids with pressure-sensitive matrices and its implications to plastic flow localization. *International Journal of Solids and Structures* 32, 3669-3691.
- Jeong, H.-Y., 2002. A new yield function and a hydrostatic stress-controlled void nucleation model for porous solids with pressure-sensitive matrices. *International Journal of Solids and Structures* 39, 1385-1403.
- Karafillis, A. P., Boyce, M. C., 1993. A general anisotropic yield criterion using bounds and a transformation weighting tensor. *Journal of the Mechanics and Physics of Solids* 41, 1859-1886.

- Lee, Y. K., Ghosh, J., 1996. The significance of J_3 to the prediction of shear bands. *International Journal of Plasticity* 12, 1179-1197.
- Logan, R. W., Hosford, W. F., 1980. Upper-bound anisotropic yield locus calculations assuming $\langle 111 \rangle$ -pencil glide. *International Journal of Mechanical Sciences* 22, 419-430.
- Maji, A. K., Schreyer, H. L., Donald, S., Zuo, Q., Satpathi, D., 1995. Mechanical properties of polyurethane-foam impact limiters. *Journal of Engineering Mechanics* 121, 528-540.
- Mendelson, A., 1968. *Plasticity: Theory and Application*. Macmillan, New York.
- Nusholtz, G. S., Bilkhu, S. S., Founas, M., Uduma, K., Debois, P. A., 1996. Impact response of foam: the effect of the state of stress. SAE Technical Paper 962418, Society of Automotive Engineers, Warrendale, Pennsylvania.
- Pan, T., Wang, J., Oh, S., Pan, J., 2002. Polymeric structural foams for light weight automotive body structures. *Proceedings of 34th International SAMPE Technical Conference*, Nov. 4-7 2002, Baltimore, MD, p. 968.
- Patel, M. R., 1969. The deformation and fracture of rigid cellular plastics under multiaxial stress. PhD thesis, University of California, Berkeley, California.
- Puso, M. A., Govindjee, S., 1995. A phenomenological constitutive model for rigid polymeric foam. MD-Vol. 68/AMD-Vol. 215, *Mechanics of Plastics and Plastic Composites*, American Society of Mechanical Engineers, New York, New York, 159-176.
- Rizzi, E., Papa, E., Corigliano, A., 2000. Mechanical behavior of a syntactic foam: experiments and modeling. *International Journal of Solids and Structures* 37, 5773-5794.
- Rockafellar, R. T., 1970. *Convex analysis*. Princeton University Press, Princeton, New York.
- Schreyer, H. L., Zuo, Q. H., Maji, A. K., 1994. Anisotropic plasticity model for foams and honeycombs. *Journal of Engineering Mechanics* 120, 1913-1930.

- Shaw, M. C., Sata, T., 1966. The plastic behavior of cellular materials. *International Journal of Mechanical Sciences* 8, 469-478.
- Triantafillou, T. C., Zhang, J., Shercliff, T. L., Gibson, L. J., Ashby, M. F., 1989. Yield surfaces for cellular materials under multiaxial loads – II. comparison of models with experiment. *International Journal of Mechanical Sciences* 31, 665-678.
- Tsai, S. W., Wu, E. M., 1971. A general theory of strength for anisotropic materials. *Journal of Composite Materials* 5, 58-80.
- Wang, A.-J., McDowell, D. L., 2005. Yield surfaces of various periodic metal honeycombs at intermediate relative density. *International Journal of Plasticity* 21, 285-320.
- Yamashita, K., Wakamori, T., Miyamoto, M., Mori, M., 1997. Application of high strength polyurethane foam for improvement of body stiffness. Conference Preprint, *Materials for Lean Weight Vehicles*, The Institute of Materials.
- Yoon, J.-W., Barlat, F., Chung, K., Pourboghrat, F., Yang, D. Y., 2000. Earing predictions based on asymmetric nonquadratic yield function. *International Journal of Plasticity* 16, 1075-1104.
- Yoon, J.-W., Barlat, F., Dick, R. E., Chung, K., Kang, T. J., 2004. Plane stress yield function for aluminum alloy sheets—part II: FE formulation and its implementation. *International Journal of Plasticity* 20, 495-522.
- Zaslowsky, M., 1973. Multiaxial-stress studies on rigid polyurethane foam. *Experimental Mechanics* 13, 70-76.
- Zhang, J., Lin, Z., Wong, A., Kikuchi, N., Li, V. C., Yee, A. F., Nusholtz, G. S., 1997. Constitutive modeling and material characterization of polymeric foams. *Journal of Engineering Materials and Technology* 119, 284-291.
- Zhang, T., Lee, J., 2003. A plasticity model for cellular materials with open-celled structure. *International Journal of Plasticity* 19, 749-770.

Table 1. The yield strengths (MPa) for the PVC foam (H200)

Hydrostatic compressive strength σ_{hc}	-3.03
In-plane equibiaxial compressive strength σ_{bc}	-2.90
In-plane uniaxial compressive strength $(\sigma_c)_1$	-2.90
Out-of-plane uniaxial compressive strength $(\sigma_c)_3$	-3.03
Axisymmetric shear strength τ_s	2.17
In-plane uniaxial tensile strength $(\sigma_t)_1$	4.15
Out-of-plane uniaxial tensile strength $(\sigma_t)_3$	4.42
In-plane equibiaxial tensile strength σ_{bt}	4.15
Hydrostatic tensile strength σ_{ht}	4.22

Table 2. The values of the fitting parameters of the function ϕ for $m = 8$ for the PVC foam (H200)

m	α	b (MPa)	$\bar{\sigma}$ (MPa)
8	0.2456	0.6385	3.4436

Table B1. The values of the fitting parameters of the function Φ for $m = 8$ for the PVC foam (H200)

m	α	a_3	b (MPa)	b_3 (MPa)	$\bar{\sigma}$ (MPa)
8	0.3850	0.9843	0.5685	0.8008	3.6184

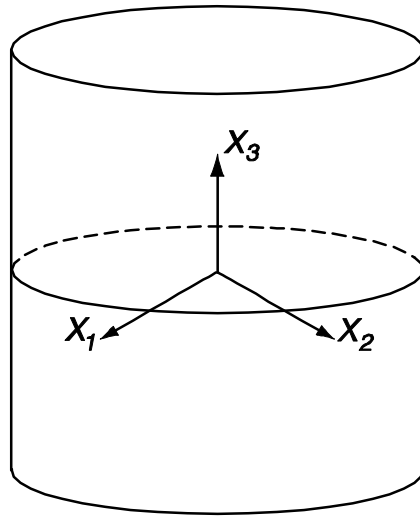


Figure 1. A circular cylindrical foam specimen and a Cartesian coordinate system.

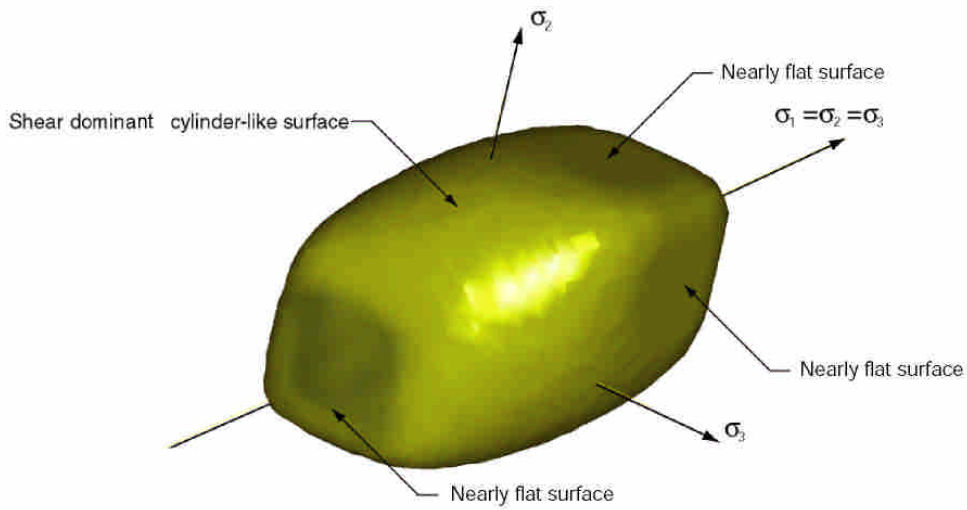


Figure 2. The yield surface based on the function ϕ in terms of the principal stresses σ_1 , σ_2 and σ_3 . Some nearly flat portions of the yield surface for $\sigma_1 > 0$, $\sigma_2 > 0$ and $\sigma_3 > 0$ and for $\sigma_1 < 0$, $\sigma_2 < 0$ and $\sigma_3 < 0$ are marked in the figure. The cylinder-like portion of the yield surface parallel to the hydrostatic stress axis $\sigma_1 = \sigma_2 = \sigma_3$ is also marked in the figure.

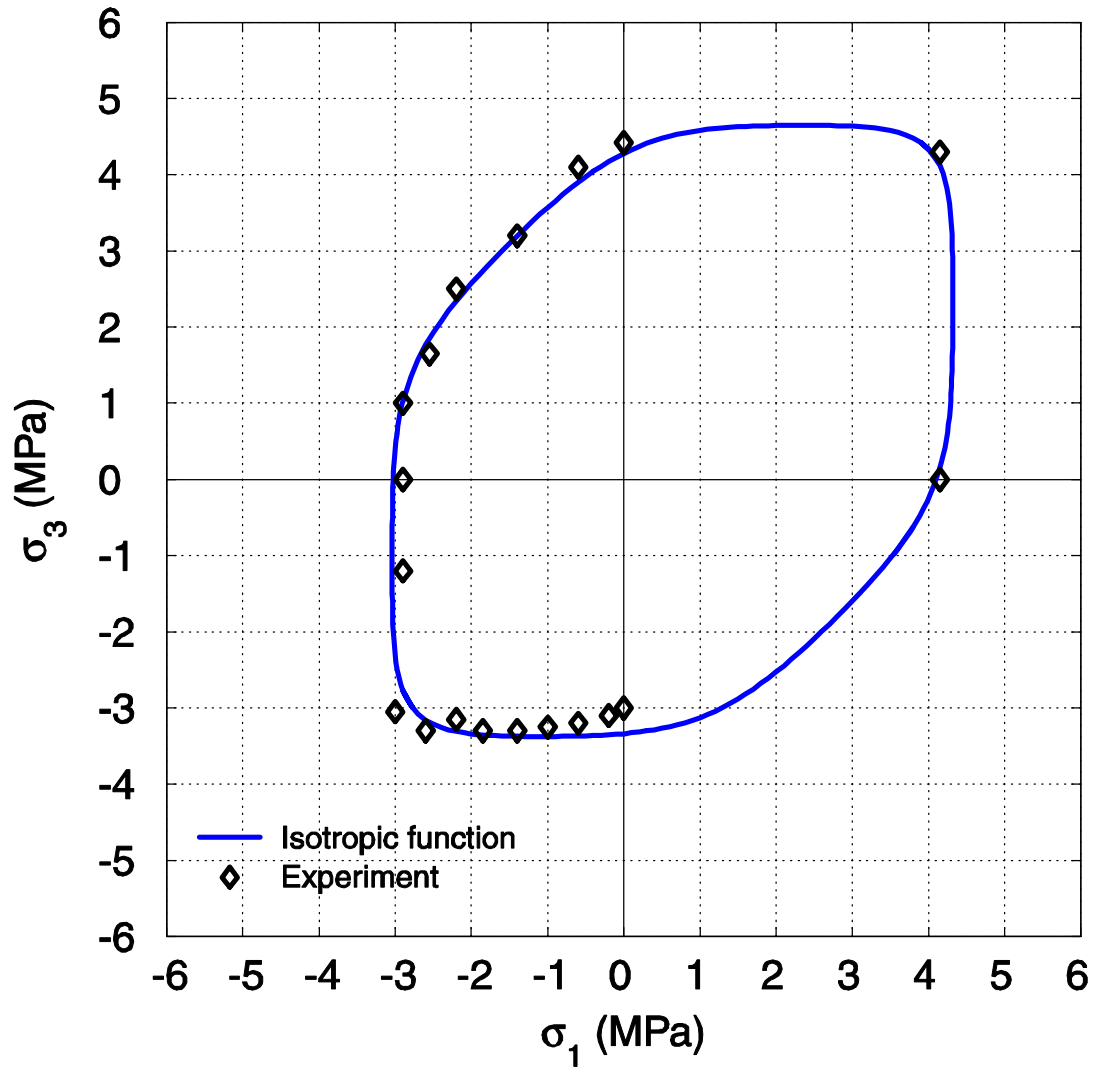


Figure 3. The yield surface based on the function ϕ and the experimental data of Deshpande and Fleck (2001) in terms of σ_1 and σ_3 .

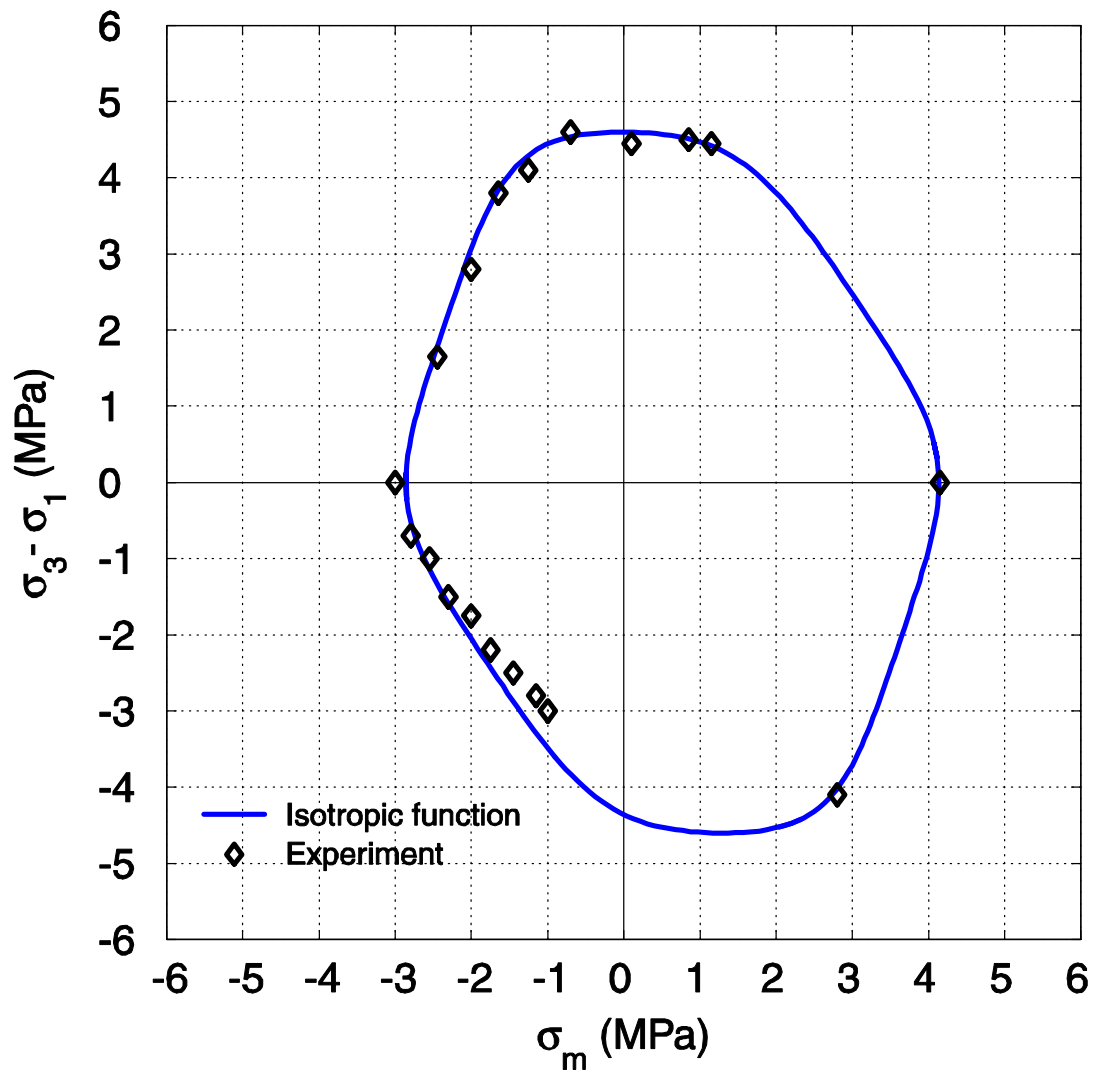


Figure 4. The yield surface based on the function ϕ and the experimental data of Deshpande and Fleck (2001) in terms of σ_m and $\sigma_3 - \sigma_1$.

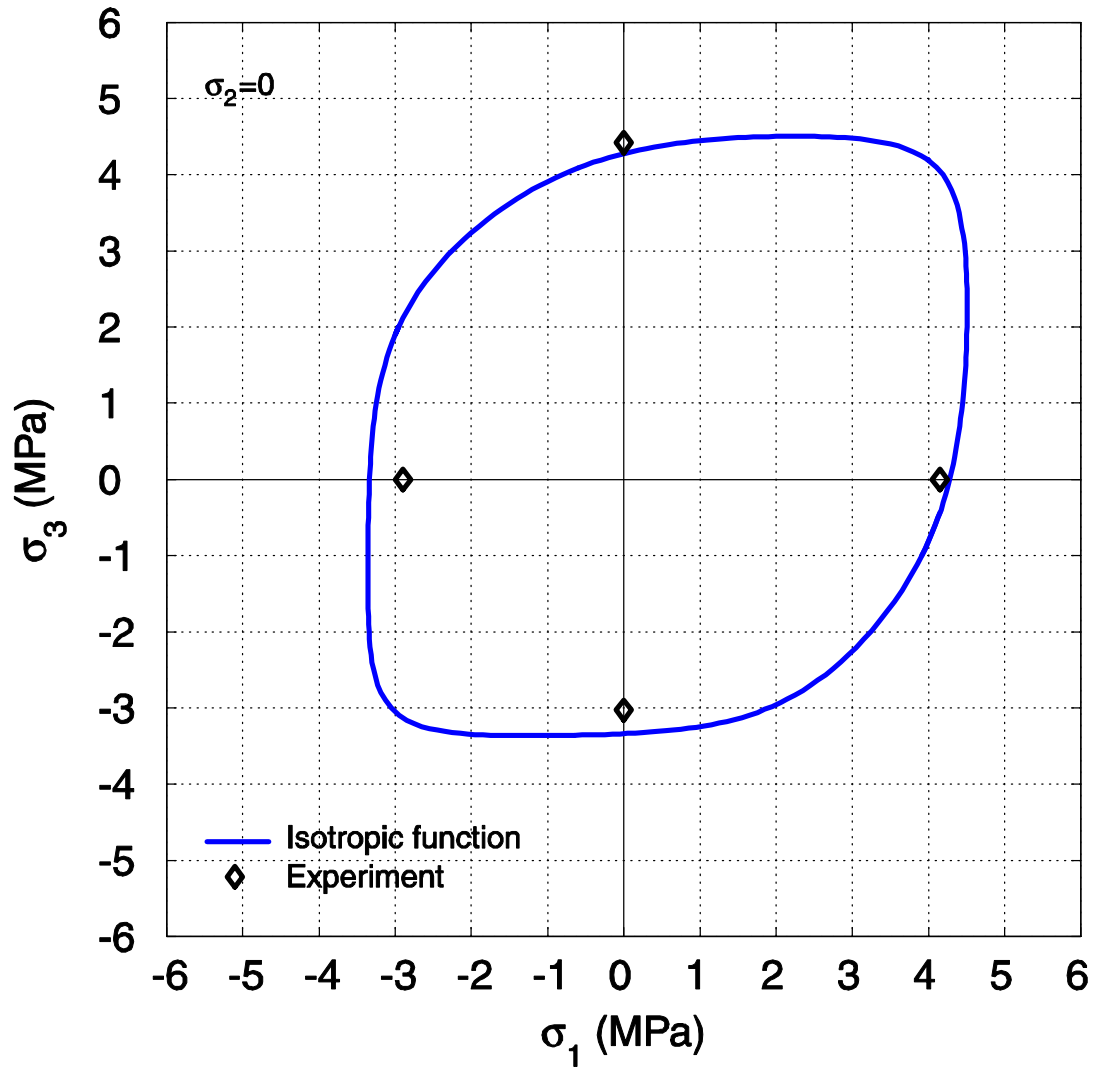


Figure 5. The yield surface based on the function ϕ and the experimental data of Deshpande and Fleck (2001) in terms of σ_1 and σ_3 in the plane of $\sigma_2 = 0$.

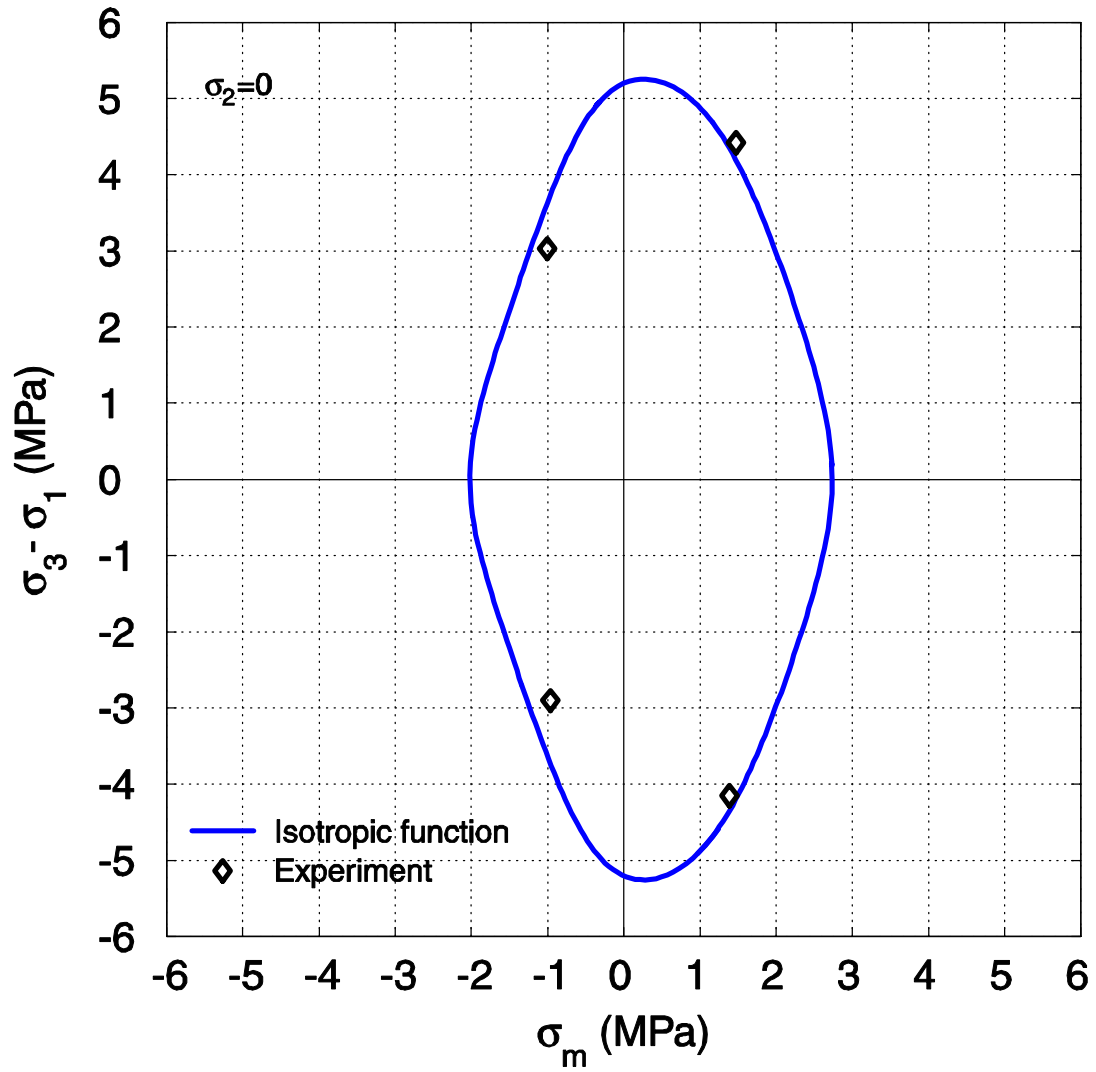


Figure 6. The yield surface based on the function ϕ and the experimental data of Deshpande and Fleck (2001) in terms of σ_m and $\sigma_3 - \sigma_1$ in the plane of $\sigma_2 = 0$.

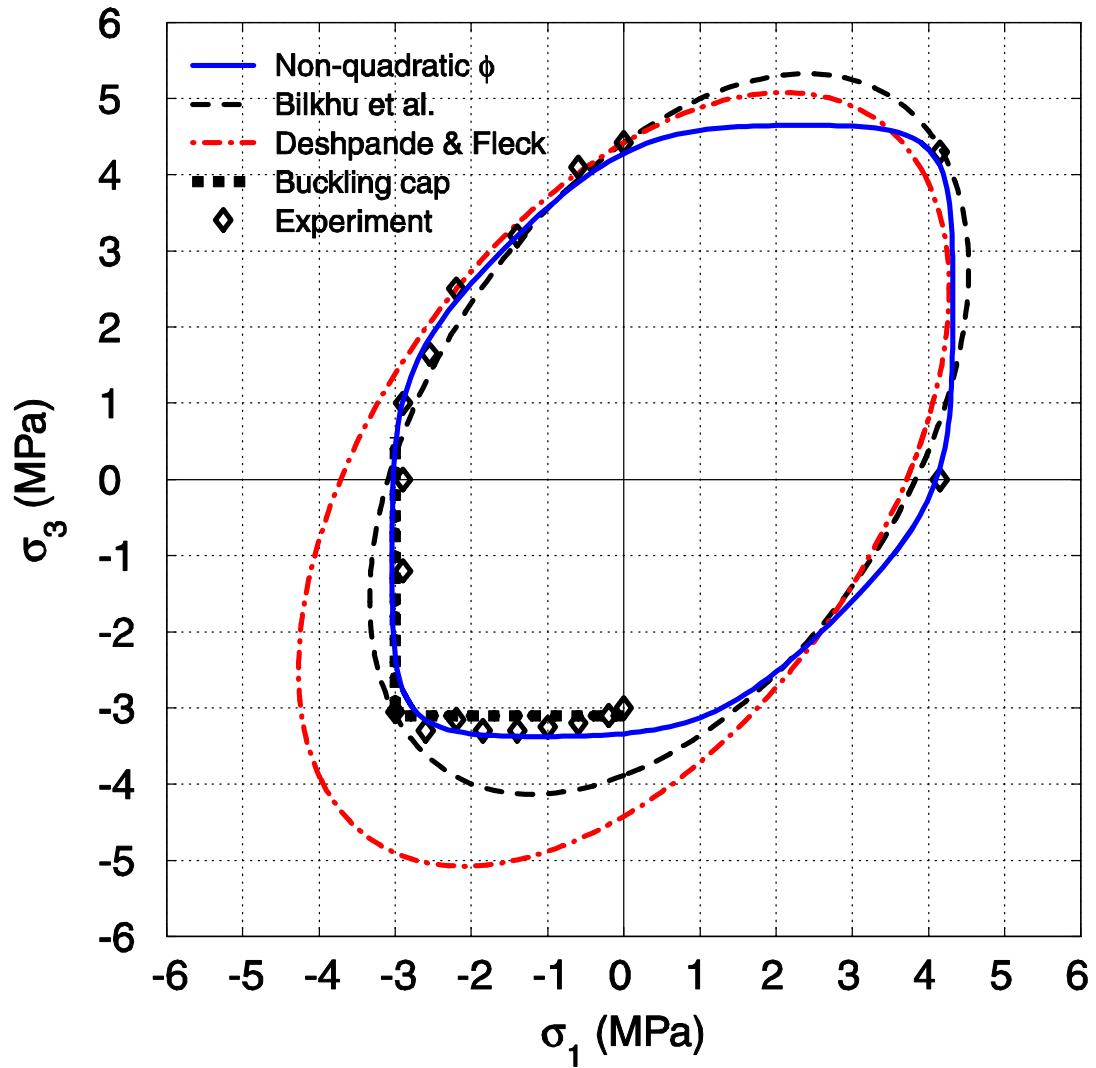


Figure 7. The experimental data of Deshpande and Fleck (2001) and the yield surfaces based on the functions ϕ_b , ϕ_d , and ϕ in terms of σ_1 and σ_3 . A buckling cap is also shown as dotted lines.

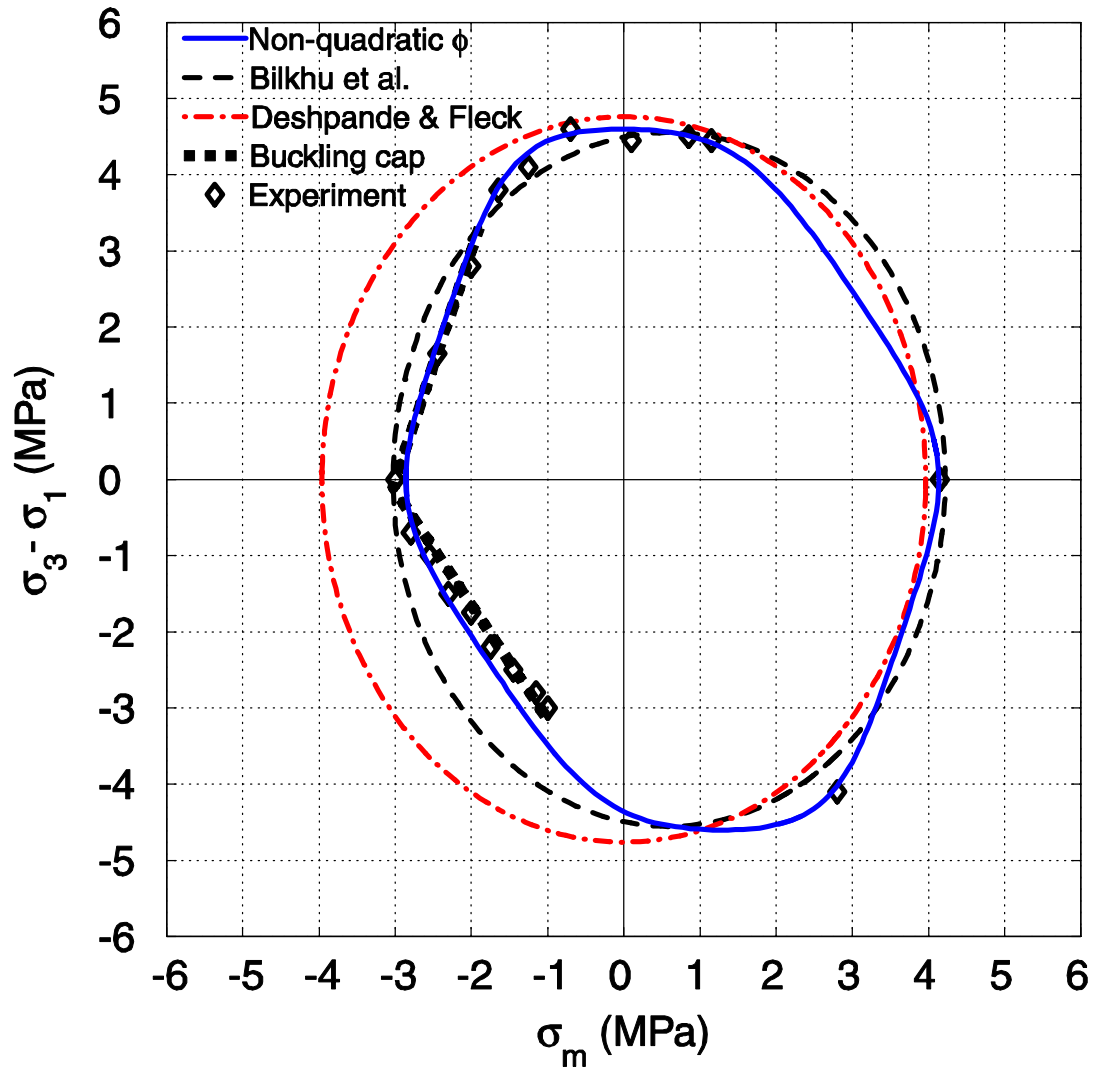


Figure 8. The experimental data of Deshpande and Fleck (2001) and the yield surfaces based on the yield functions ϕ_b , ϕ_d , and ϕ in terms of σ_m and $\sigma_3 - \sigma_1$. A buckling cap is also shown as dotted lines.

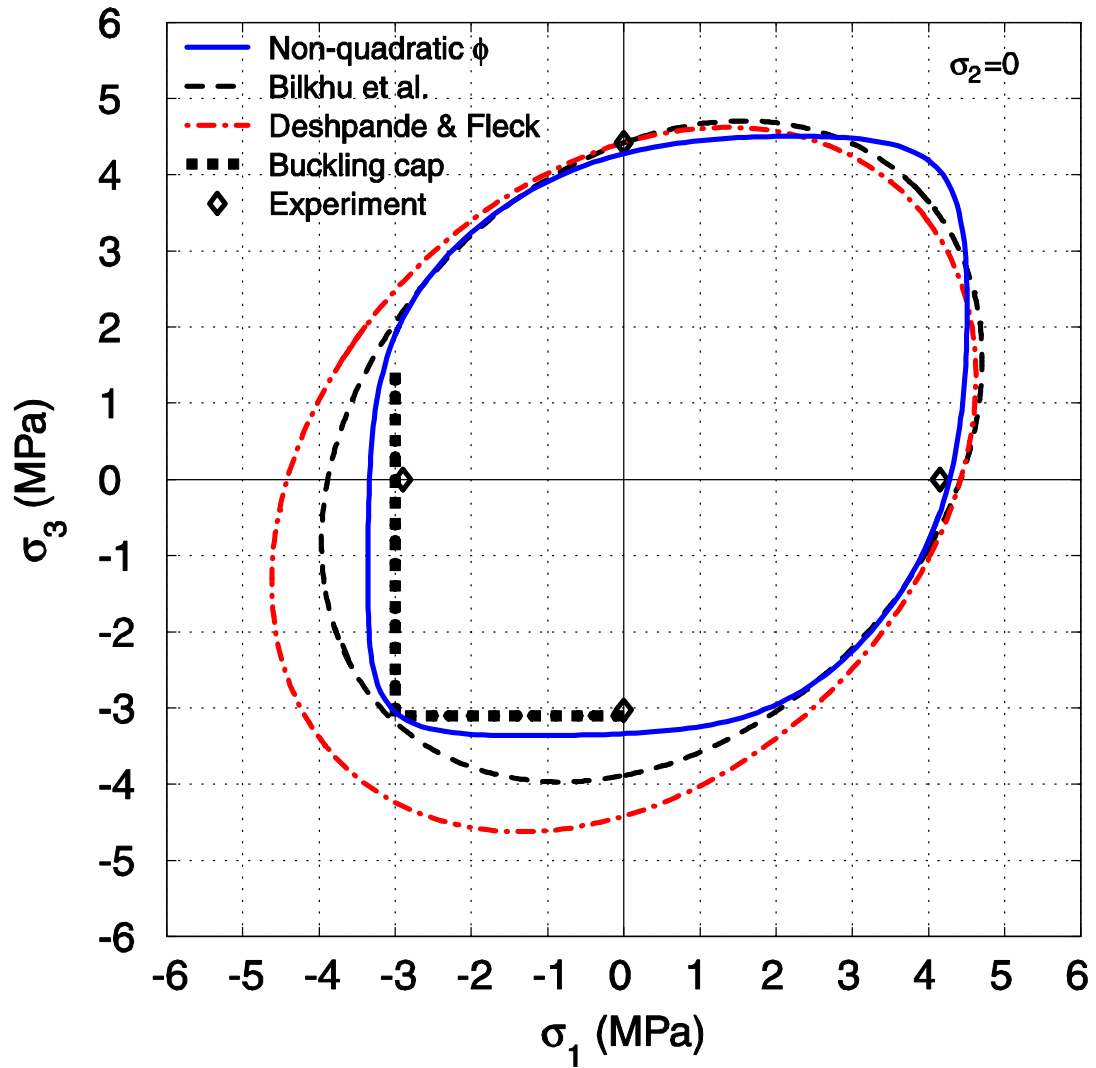


Figure 9. The experimental data of Deshpande and Fleck (2001) and the yield surfaces based on the yield functions ϕ_b , ϕ_d , and ϕ in terms of σ_1 and σ_3 in the plane of $\sigma_2 = 0$. A buckling cap is also shown as dotted lines.

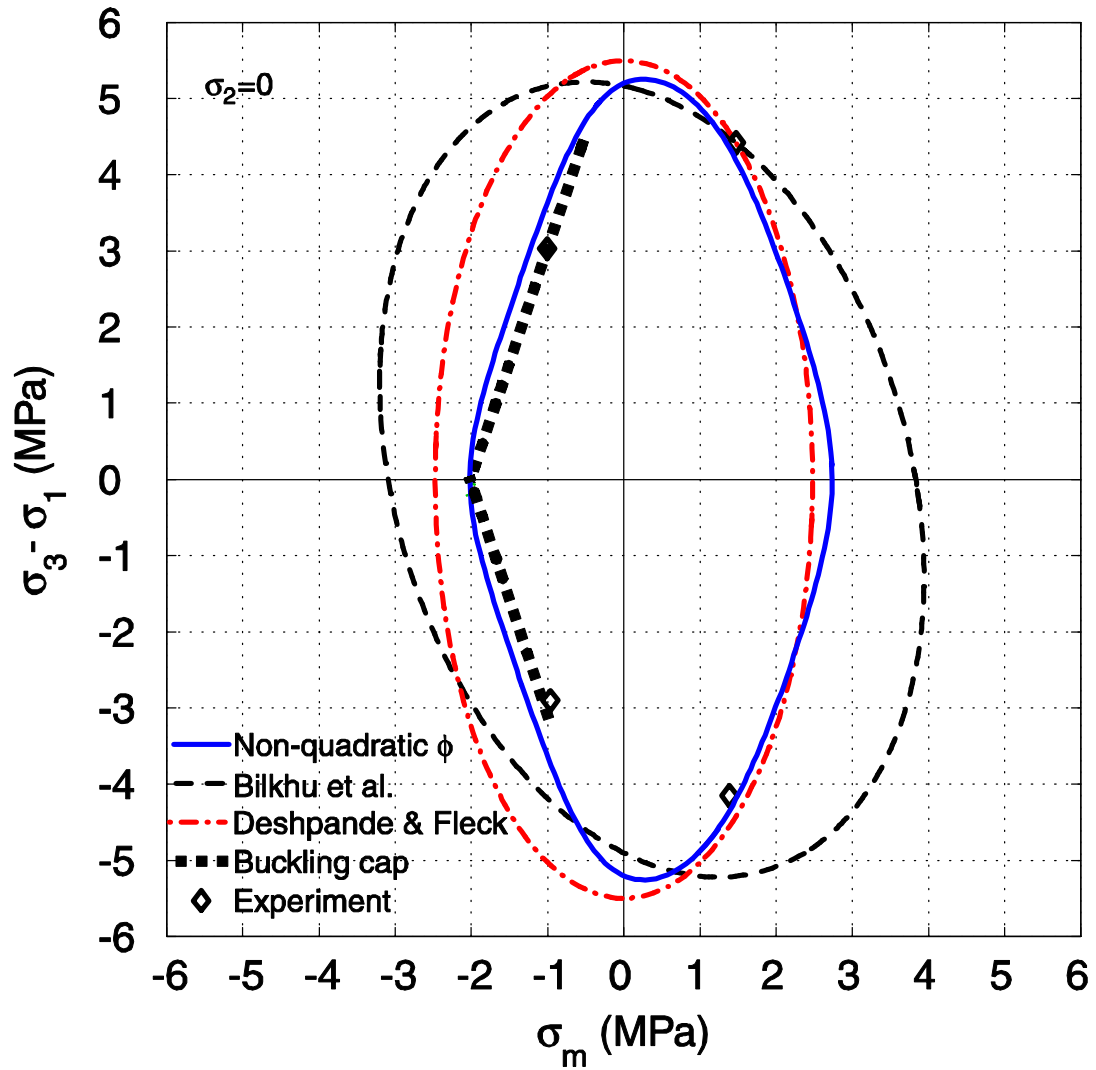


Figure 10. The experimental data of Deshpande and Fleck (2001) and the yield surfaces based on the yield functions ϕ_b , ϕ_d , and ϕ in terms of σ_m and $\sigma_3 - \sigma_1$ in the plane of $\sigma_2 = 0$. A buckling cap is also shown as dotted lines.

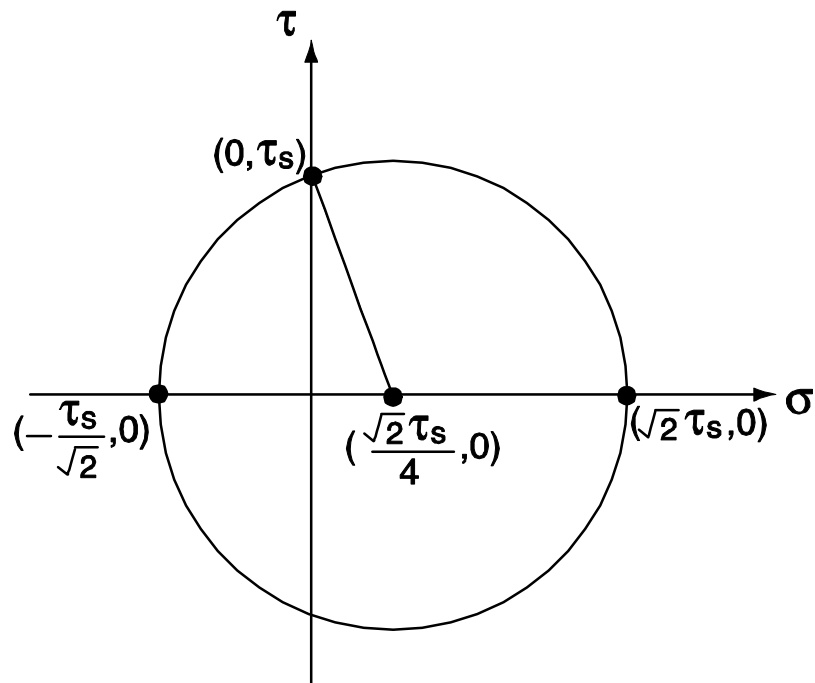
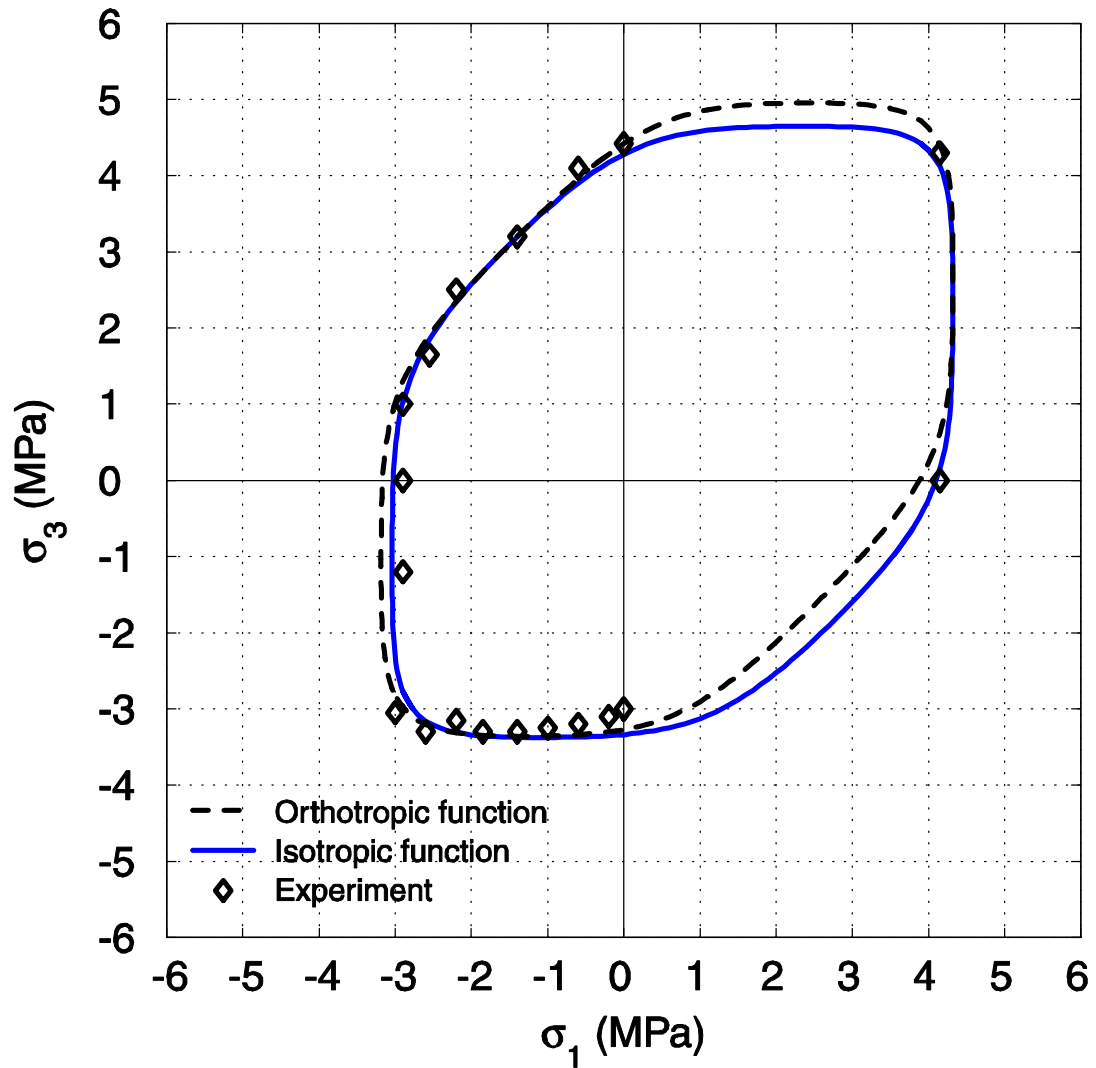
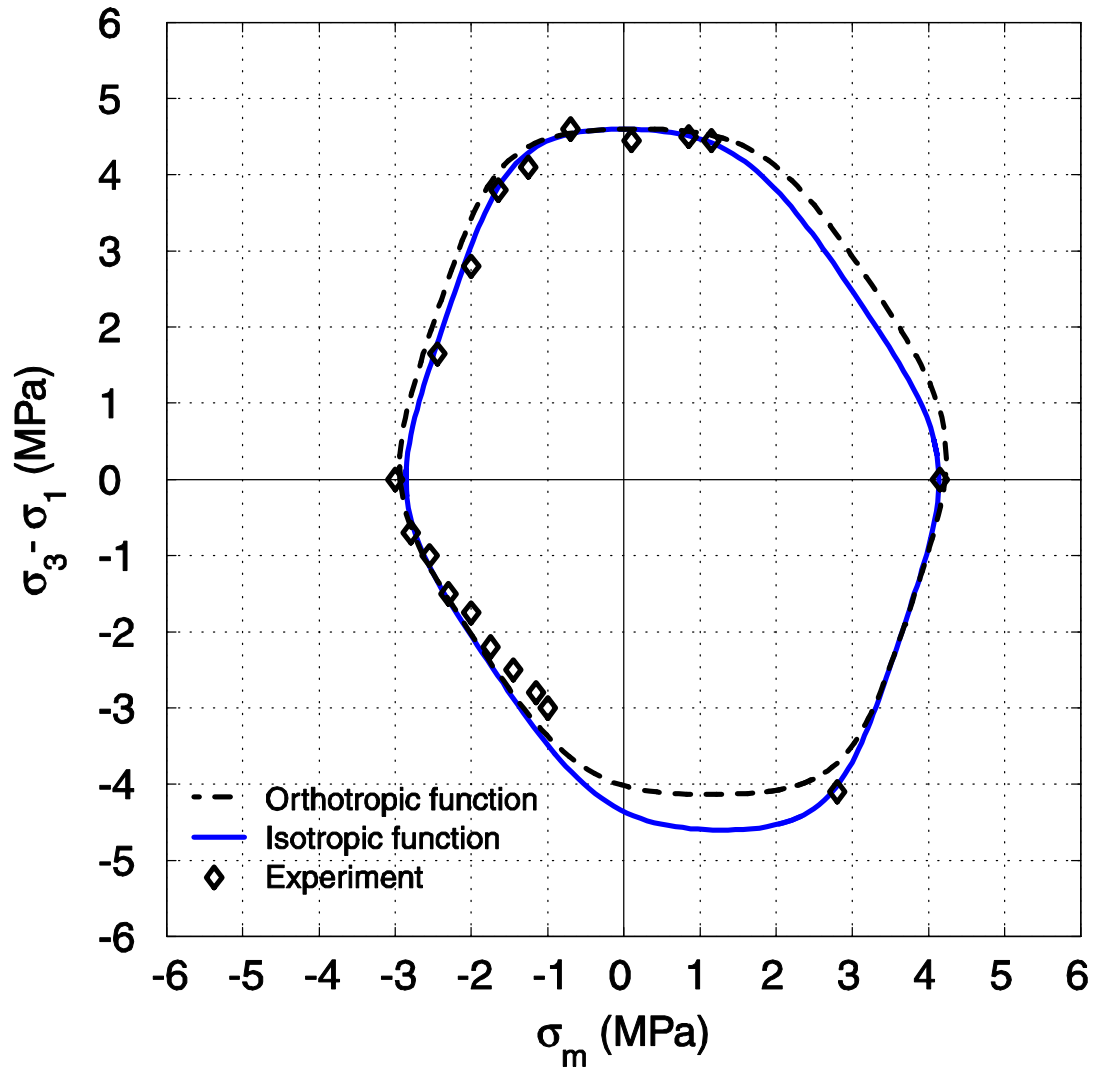


Figure A1. The Mohr circle for the case of axisymmetric shear. Here, $\sigma_1 = \sigma_2 = -\tau_s/\sqrt{2}$ and $\sigma_3 = \sqrt{2}\tau_s$ based on the conditions of $\sigma_1 = \sigma_2$ and $\sigma_1 + \sigma_2 + \sigma_3 = 0$. Note that τ_s represents the axisymmetric shear strength.





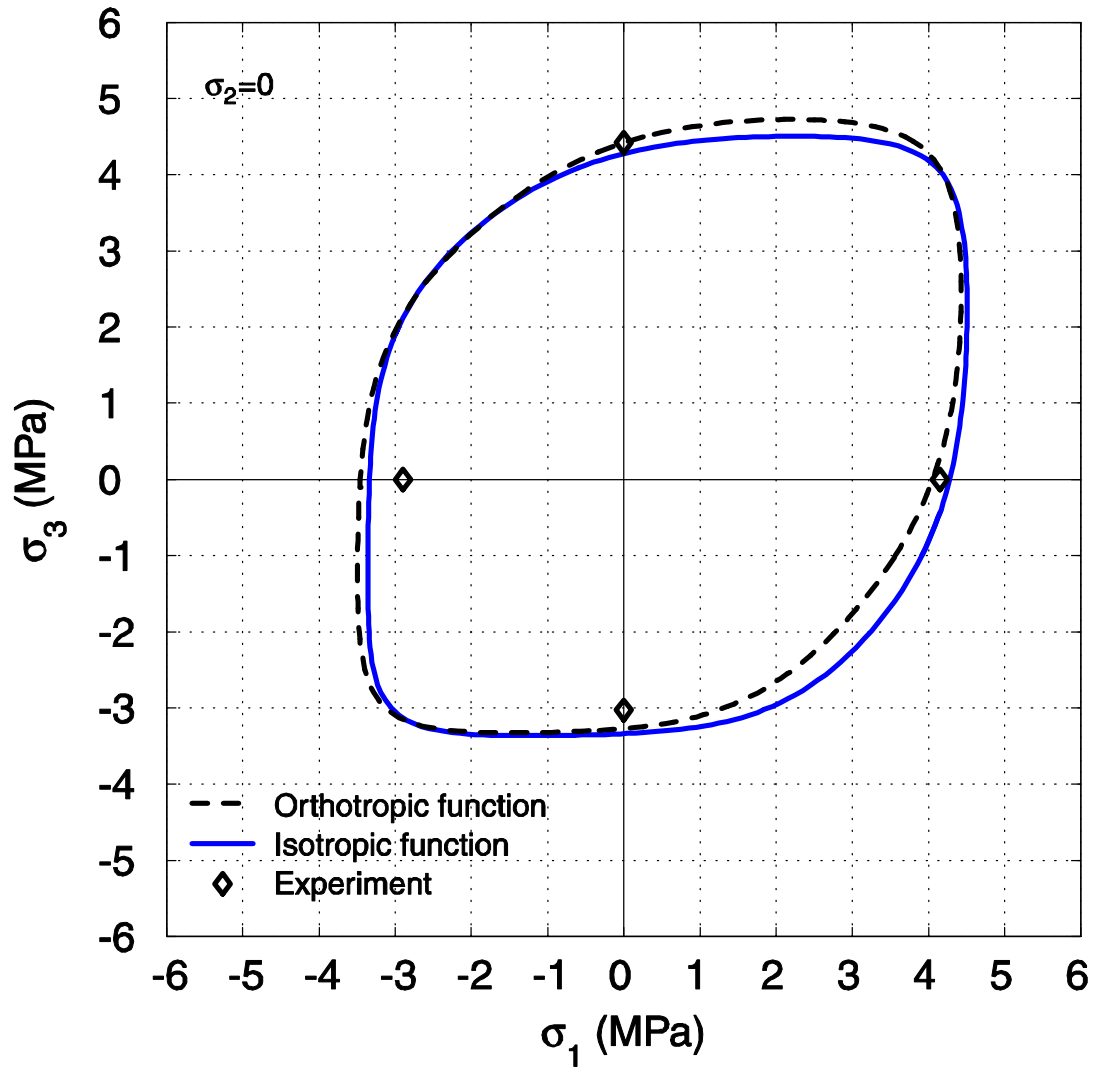


Figure B3. The yield surface based on the function Φ and the experimental data of Deshpande and Fleck (2001) in terms of σ_1 and σ_3 in the plane of $\sigma_2 = 0$. The yield surface based on the function ϕ as shown in Figure 5 is also plotted in the figure.

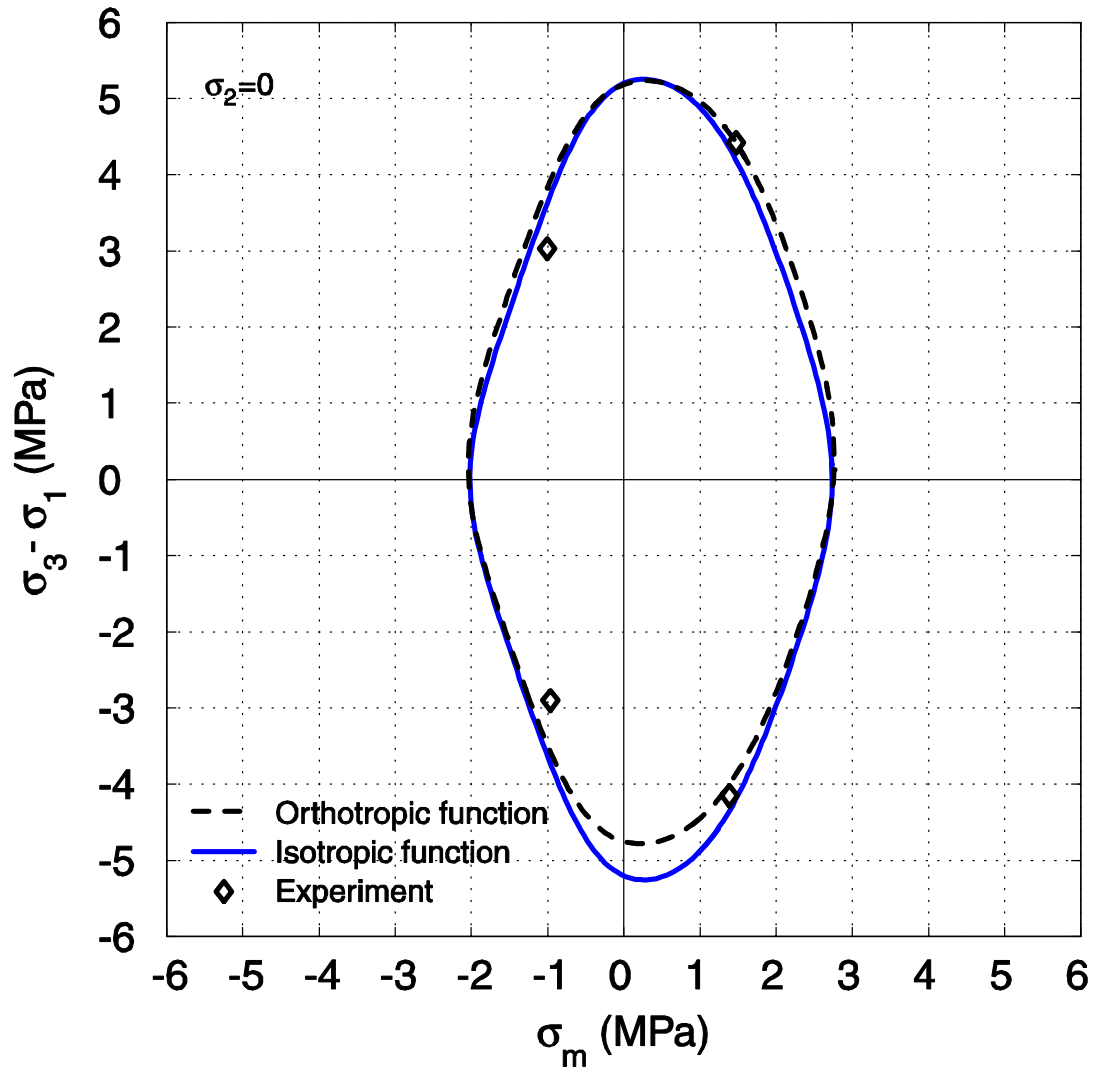


Figure B4. The yield surface based on the function Φ and the experimental data of Deshpande and Fleck (2001) in terms of σ_m and $\sigma_3 - \sigma_1$ in the plane of $\sigma_2 = 0$. The yield surface based on the function ϕ as shown in Figure 6 is also plotted in the figure.